RSC Advances

This is an *Accepted Manuscript*, which has been through the Royal Society of Chemistry peer review process and has been accepted for publication.

Accepted Manuscripts are published online shortly after acceptance, before technical editing, formatting and proof reading. Using this free service, authors can make their results available to the community, in citable form, before we publish the edited article. This *Accepted Manuscript* will be replaced by the edited, formatted and paginated article as soon as this is available.

You can find more information about *Accepted Manuscripts* in the Information for Authors.

Please note that technical editing may introduce minor changes to the text and/or graphics, which may alter content. The journal's standard Terms & Conditions and the Ethical guidelines still apply. In no event shall the Royal Society of Chemistry be held responsible for any errors or omissions in this *Accepted Manuscript* or any consequences arising from the use of any information it contains.

ROYAL SOCIETY OF CHEMISTRY

www.rsc.org/advances

Antitumor potential of the anethole singly and in combination with cyclophosphamide in murine Sarcoma-180 transplantable tumor model.

Samarjit Jana[1], Kartick Patra[1], Gopeswar Mukherjee[2], and Shamee Bhattacharjee[1*], Deba Prasad Mandal[1*].

[1]Department of Zoology,
West Bengal State University,
Berunanpukuria, Malikapur,
North-24 Parganas, Barasat,
Kolkata-700126, West Bengal, India.

[2]Department of Pathology,
Barasat District Hospital,
Barasat, North-24 Parganas,
Kolkata- 700124, West Bengal, India.

*** To whom correspondence should be addressed**

Mobile: ***91-9831479164, 91-9830505042;*** **Fax: 91-033- 254-1977;**

E-mail : dpmandal1972@gmail.com; shamee1405@gmail.com,

Funding : This work has been funded by the Council for Scientific and Industrial Research (CSIR), Govt. of India (Scheme No. 37(1487)/11/EMR-II).

RSC Advances Accepted Manuscript

ABSTRACT

The clinical outcome of chemotherapy in cancer treatment is limited due to severe side effects. There has been a mixed response in experimenting with combination of conventional chemotherapy with dietary agents to improve therapeutic outcome. The study was aimed to explore the anti-tumor potential of a spice-derived phytochemical, anethole singly and in combination with cyclophosphamide. Various doses of anethole (10, 20 and 40 mg/kg) was administered orally on alternate days to sarcoma-180 solid tumor bearing Swiss albino mice on appearance of palpable tumor. Cyclophosphamide (100mg/kg) was injected into anethole treated or untreated tumor bearing mice for 3 consecutive days before sacrifice. Results demonstrated that anethole and cyclophosphamide, singly as well as in combination, reduced tumor load to a significant extent. Cell cycle analysis revealed that cyclophosphamide and cyclophosphamide+anethole exhibited significantly more tumoricidal activity than anethole alone. AnnexinV/PI assay suggested that necrosis was the principal means of tumor reduction when cyclophosphamide was used alone or in combination contrasting to the induction of apoptosis in anethole groups. The necrotic cell death was also reflected in tumor histology. Although no additive effect in tumor reduction was observed with combinatorial treatment, but use of anethole was instrumental in reducing the side-effects namely myelosupression, hepatotoxicity and urotoxicity of cyclophosphamide treatment. The hepatoprotective effect of anethole was further proven by its ability to reduce CCl_4 induced hepatotoxicity. This study indicates that anethole pre-treatment protected the bone marrow, liver and urinary bladder from the toxic side-effects of cyclophosphamide without interfering with its anticancer effect.

Key Words: Anethole, Cyclophosphamide, anticancer, apoptosis, necrosis, side-effects

RSC Advances Accepted Manuscript

INTRODUCTION

Chemotherapy of cancer has evolved considerably in the past few decades leading to improvements in the treatment of different malignancies. With the advent of aggressive chemotherapy, however, incidences of adverse side-effects in cancer patients have also increased[1]. These anticancer drugs not being target specific, also damage healthy cells, especially those with rapid turnover such as gastrointestinal, hematopoietic and immune cells[2]. Thus, often it is seen that though a chemotherapeutic agent or regime successfully counters tumor growth, the treatment is abrogated principally because of severe toxic side effects[3]. The toxic side-effects of anticancer drugs can be a major limitation to the clinical efficacy of various chemotherapeutic regimens. Moreover, treatment of solid tumors by conventional chemotherapy is still a formidable challenge. Solid tumors are generally resistant to chemotherapy due to the inability of the drugs to access hypoxic region[4]. This attenuated success with conventional chemotherapy creates scope for the exploration of safer and more effective alternative treatment approaches. Natural product repertoire is a potential source for novel drugs. Especially important in this regard are the naturally occurring phytochemicals present in foods such as vegetables, fruits, spices and plant roots[5]. This knowledge has inspired the use of plant products as complementary and alternative therapies both as direct and adjuvant remedy. A growing body of literature suggests the cancer preventive and therapeutic potential of phytochemicals[6,7] and a lot of research has focused on the cellular mechanisms by which these phytochemicals interfere with the carcinogenic process[8]. With the ability to target a variety of signaling pathways, phytochemicals are considered to be promising therapeutic agents against tumors with limited toxicity to normal cells. In addition, many studies have reported that phytochemicals can sensitize cancer cells to conventional cytotoxic agents. Thus, phytochemicals can exert their anticancer effect either in monotreatment or in association with conventional chemotherapeutic agents as co-chemotherapeutic drugs.

RSC Advances Accepted Manuscript

In view of this, here we have made an attempt to elucidate the anticancer potential of the spice-derived phytochemical, anethole, as single anticancer agent and/or in association with a conventional chemotherapeutic agent, cyclophosphamide. Anethole, 1-methoxy-4-(1-propenyl) benzene, is the major component in anise oil, fennel oil, and camphor[9] and is known to exhibit antioxidative, chemopreventive, anticarcinogenic and anti-inflammatory properties[10]. Recently a few studies have also stressed on the anti-metastatic and pro-apoptotic activity of this spice-derived phytochemical. However, all these activities have been studied *in vitro* in cancer cells[11-14] without proper *in vivo* experimentations. Till date there is only one report on the anticancer effect of anethole *in vivo* in a murine carcinoma model[15].

There were two major objectives of the present study: First, to elucidate the *in vivo* anti-cancer potential of anethole and secondly, to investigate whether pretreatment with anethole increases the efficiency of the conventional anticancer drug, cyclophosphamide (cyclo).

To test our objectives we have investigated the effect of anethole in Sarcoma-180 (S-180) transplantable tumor model in Swiss albino mice. It is generally believed that combinations of cytotoxic agents with phytochemicals retard cancer growth more effectively than when used singly[16]. Hence, in this study, we have also tested whether or not anethole together with, cyclo, can inhibit tumor growth more effectively than anethole or cyclo alone and/or is able to overcome the non-specific cytotoxicity of conventional chemotherapy towards normal cells.

RESULTS

Anethole inhibits tumor growth in S-180 tumor bearing mice

Measurement of tumor weight after the experimental duration showed that anethole caused a dose-dependent reduction in tumor weight as compared to the sarcoma control group. The tumor weights recorded were 4.40±0.215, 3.69±0.56 and 2.94±0.27 gms for

RSC Advances Accepted Manuscript

the anethole 10, 20 and 40 respectively as compared to 5.63±0.44gm in the sarcoma control group (Fig. 1 A).

Histopathological evaluation of the tumor tissues also showed diffused zones of necrosis caused by anethole treatment as compared to the untreated tumors (Fig 1B).

Anethole induces apoptosis in S-180 cells

To ascertain and quantify the nature of cell death brought about by anethole, we performed comet and Annexin V/PI assay in the tumor cells. Apoptosis was confirmed by both the experiments and a dose dependent occurrence of the phenomenon was observed. As compared to a negligible 3.0%±1.5 annexin positive cells in the sarcoma control tumors, treatment with anethole 10, 20 and 40 caused an increase of 18.77%±1.17, 48.16%±0.6 and 62.8%±3.7 respectively (Fig. 2A&B). The low occurrence of PI positive cells in all the anethole treated groups reveals that necrosis was not a significant player in reducing the tumor load (Fig. 2B). The phenomenon of apoptosis was further confirmed by 'comet assay' showing halo around the nucleus and a consequent decrease in nuclear DNA content[17](Fig. 2C&D).

Effect of Anethole on other organs

After testing the antitumor potential of anethole, we examined its side effects, if any, on vital organs viz. liver, kidney and bone marrow. Histopathological analysis of liver (Fig. 3A&B) and kidney (Fig. 3D&E) suggests a dose dependent increase in the toxic manifestations of anethole. Measurement of hepatic LPO showed an increased oxidative stress in liver (20.2±2.07) by the highest dose of anethole as compared to the normal liver (9.4±1.24) (Fig.3C). Interestingly, anethole 40 was not found to be toxic to the bone marrow (Fig. 3F). As anethole was dissolved in 50% alcohol (administered 50µl per dose), its effect on liver and kidney was also studied. However, no notable or significant change was noticed in any of the parameters (Fig. 3A-E).

In the next phase of experiments, the effect of combinatorial treatment with cyclophosphamide and different doses of anethole was studied.

RSC Advances Accepted Manuscript

Effect of combination treatment on S-180 tumor growth

Fig. 4A&B reveals the comparative reduction of tumor load by treatment with cyclo singly or in combination with anethole as compared to sarcoma control. The tumor weight did not show much variation in the different treatment groups recording 2.96±0.18gms, 3.16±0.185gms, 2.82±0.07 and 2.69±0.265 in the cyclo and consecutive combination groups respectively. However all the treatments yielded significant decrease in tumor mass as compared to sarcoma control group (5.63± 0.44gm). A similar trend was also observed in case of tumor volume reduction.

The significant reduction in tumor mass was also evident from tumor histopathological assessment which revealed extensive zones of necrosis (Fig. 4C) in all the treatment groups. Interestingly, however, the necrotic zones were far more in the cyclo and combination groups than in anethole only treated groups (Fig.1B). This inspired us to look more deeply into the nature of tumoricidal activity of the different treatment regimes.

Differential modes of cell death induced by the different treatment regimes

Despite causing similar reduction in tumor weight and volume, cell cycle analysis of S-180 cells isolated from tumor tissues of various treatments groups reflected a different picture. All the treatment groups yielded significantly greater hypoploid tumor cell population than the sarcoma control group, the highest proportion being recorded in the combination groups (Fig.5 A&B). To further expand on the nature of cell death induced by each of the treatment regimes, we performed Annexin V/PI assay. Interestingly, anethole 20 yielded the greatest population of annexin positive cells (48.11%±0.6) as compared to 10.47%±3.11 in cyclo and 20.7%±0.91, 37.6%±3.13 and 17.98±1.6% in the consecutive combination groups. PI positive cells were, however significantly more in the cyclo (67.17%±2.63) and combination groups (52.93%±1.83, 42.87%±1.42 and 66.9%±1.49 respectively in cyclo+anethole10, 20 and 40) (Fig.5C-E). Except cyclo+anethole10, in terms of total killing, the other two combinations were more

RSC Advances Accepted Manuscript

effective than cyclo. However, all doses of anethole combined with cyclo yielded superior tumoricidal activity than administration of the phytochemical alone.

Effect of combination treatment on tumor tissue protein expressions

In order to elucidate the molecular mechanism of the cell death induced by various treatment regimes, we detected the expression of some protein markers of cell death and proliferation in the tumor tissues. Expression of proteins p53, p21 and cleaved PARP-1 was almost identical in the cyclo and combination groups (Fig. 6A-C). Pro-apoptotic Bax caspase-3 and caspase-8 expression (Fig. 6D, G, H) was higher in cyclo+anethole combination followed by anethole 20, 40 and then cyclo. Consequently, Bax/Bcl-2 ratio (Fig.F) was also found to be higher in the cyclo+anethole treated tumor tissues followed by anethole 20 and 40 which probably is consistent with the higher percentage of apoptotic cells in these groups than the cyclo group. Simultaneously, expression of the proliferation marker PCNA was considerably downregulated in all treated groups with the highest reduction being observed in the combination groups (Fig. 6I). Equal loading of protein was confirmed by GAPDH expression (Fig.6J).

Effect of combination treatment on myelosuppression, hepatotoxicity and Urotoxicity

Having confirmed the antitumor effect of cyclo+anethole, we proceeded to investigate whether or not combinatorial regime could moderate the myelosuppressive, hepatotoxic and urotoxic effect of cyclo.

According to Fig. 7A-B, combination treatment could recover the depression in bone marrow cell population to a significant extent as compared to cyclo. The huge hypoploidy peaks in cyclo treated groups (52.55%±0.098) could be successfully contained to 45±0.34, 34±0.23 and 35±0.67 with cyclo+anethole 10, 20 and 40 treatment respectively. The ameliorative effect of anethole on bone marrow is also reflected in the results of comet assay (Fig.7C&D).

RSC Advances Accepted Manuscript

Hepatic histopathological assessment (Fig.7E&F) and liver function test (Table 1) from treated and control groups reveal that anethole pre-treatment reduced cyclo-induced hepatic stress. As anethole 20 provided maximum protection to the liver, this dose was selected for further study on its effect against carbon tetrachloride (CCl_4) induced hepatotoxicity. Pretreatment with anethole 20 significantly lowered the degree of CCl_4 induced hepatic necrosis as compared to carbon tetrachloride administered singly (Fig. 7G&H). The significant increase in the serum biomarkers of hepatotoxicity with CCl_4 treatment was also considerably reduced by anethole pre-treatment (Table 1). This confirms the hepatoprotective effect of anethole. Comet assay also fortified the histopathology findings. (Fig7 I&J)

Cyclo is known to induce haemorrhagic cystitis, necrosis and edema to the urothelium during its excretion. Combining anethole with cyclo could effectively reduce the degenerative changes in the transitional epithelium and inflammation induced by the latter as can be seen in the histology sections of the urinary bladder of different experimental groups (Fig.7K&L). Renal function test results also support this observation (Table 2).

DISCUSSION

This study was conducted to investigate the *in vivo* antitumor potential of the spice-derived phytochemical anethole in a murine transplantable tumor model. Moreover, in this study we have also explored the effect of various doses of anethole in combination with a widely used chemotherapeutic agent cyclophosphamide. Several studies suggest that phytochemicals from dietary plants are important as adjuvant therapy conjunction with conventional chemotherapy to contain the adverse side effects of the latter[18]. On the other hand, there are also arguments against using dietary supplements during chemotherapy because they supposedly interfere with the cytotoxicity of chemotherapeutic agents[19].

Though the anticancer property of anethole has been documented in a few earlier studies[20] and one study has also reported the synergism of anethole with platinum drugs against cancer[21], however, all of these are in vitro studies which need to be confirmed in vivo.

RSC Advances Accepted Manuscript

Results obtained from the present study demonstrate that treatment with cyclo or anethole singly and in combination reduced the tumor volume and weight significantly as compared to the untreated tumor bearers. Despite identical reduction in tumor load in cyclo and the various combination groups, data from tumor histology, cell cycle and annexin assay suggests that combination treatment was more effective. The apparent contradiction in the extent of tumor volume reduction and percentage cell death induced by cyclo and combination treatment regime in this study is in line with earlier studies which have reported discrepancies between volume change and histopathological assessments[22,23].

Another interesting observation as revealed by the results of AnnexinV/PI assay in this study is the increased apoptotic induction by anethole treatment and necrosis by cyclo. In all the combination groups also, there is a distinct shift in the population of cells from necrosis to apoptosis. It is generally considered that apoptotic cell death is less harmful than necrosis as the former process minimizes inflammatory reactions[24]. The shift in the cell death from predominantly necrosis in cyclo to apoptosis in the combination and phytochemical only treatment regime might be due to a reduction in oxidative stress by anethole treatment[25]. In similar lines with this finding, an earlier study provided the first in vivo evidence of a shift from necrosis to apoptosis without reducing total cell death following GSH administration[26]. Thus, in the present study, induction of cell death, both in terms of nature as well as quantity, is different among the various treatment groups. Administration of cyclo together with anethole exhibited higher antitumor activity than cyclo or corresponding anethole doses administered singly. However, no synergistic or additive antitumor effect was observed in the combination groups.

Consistent with the higher anticancer activity in the combination groups, expression of the apoptotic marker Bax and the Bax/Bcl-2 ratio and caspase-8 expression was higher in cyclo+anethole 20 and 40 groups as compared to cyclo. There are studies which have reported that apart from inducing apoptosis by the extrinsic pathway, caspase-8 inhibits

RSC Advances Accepted Manuscript

necrosis[27-29], which plausibly explains the decreased percentage of necrotic cells in this group as compared to the other experimental groups. Expression of other proteins like p53, p21[30], caspase-3[31] and cleaved PARP-1[32] which can be implicated both in apoptotic as well as necrotic cell death mechanisms, was, however, correlative to death induction rather than to the phenomenon of apoptosis.

Exploration of the effect of these treatments on other organs suggested that the advantage of anethole pre-treatment, also lies in its ability to reduce cyclo induced adverse side-effects, viz. myelosuppression, hepatotoxicity and urotoxicity. Histopathological scoring of liver tissue indicates that anethole was able to protect the hepatocytes from the toxic effect of cyclophosphamide. The hepatoprotective effect of anethole was reaffirmed by its ability to ameliorate CCl_4 induced hepatotoxicity. It is reported that hepatocyte death is the main event that leads to liver injury[33]. Results of comet assay in liver cells suggested increased cyclo induced hepatocyte death. This could be prevented by treatment with anethole administered either singly or in combination as compared to the control or cyclo treated groups. The significant suppression in bone marrow was also restored in the cyclo+anethole groups suggesting the protective effect of anethole on the primary lymphoid organs as well. Cell cycle analysis revealed that the marked increase in the hypoploid region of bone marrow cells due to cyclo treatment was significantly restricted by combining it with anethole.

It is known that the toxicity of cyclo is induced mainly by oxidative stress[34]. There are various studies which support the notion that chemotherapy induced toxicity may be moderated by administration of antioxidants[35]. Anethole has been shown to possess antioxidant activity by many authors[36-37]. Therefore, the protective effect of anethole against cyclo-induced toxicity may be due to its antioxidant activity.

Amongst all the treatment regimes, cyclo+anethole20 combination was found to be the most effective both in terms of its ability to ameliorate cyclo induced toxicity to vital organs as well as its tumoricidal action.

RSC Advances Accepted Manuscript

EXPERIMENTAL

Reagents and materials

Annexin V-FITC Kit was purchased from (Biovision, USA), Anti-mouse anti-bodies against p53, p21, Bax, Bcl-2, caspase-3, caspase-8, Poly (ADP-ribose) polymerase (PARP-I), PCNA, were procured from Santa Cruz Biotechnology (USA). Trans-Anethole (97% pure; Sigma Aldrich, St. Louis, MO), cyclophosphamide, Carbon-tetrachloride, 1-chloro-n inhibitor, bacitracin, leupeptin, pepstatin A, PMSF, phos-phatase inhibitor cocktails, RNase and NBT were purchased from Sigma (St. Louis, MO). NP-40 was purchased from Merck Germany. The supported nitrocellulose membrane, and filter papers were obtained from Gibco BRL, USA and Millipore, USA respectively. The remaining chemicals and materials were purchased from local firms (India) and were of highest grade.

Animal model

Male Swiss albino mice were maintained in plastic cages (~6 mice / cage) at an ambient temperature of 22-25˚C on a 12 hour light / dark cycle with access to drinking water and pellet diet (NIN, Hyderabad, India) *ad libitum*. All the animal experimentations were approved by the Institutional Animal Ethical Committee (IAEC), registered under Committee for the Purpose of Control and Supervision of Experiments on Animals (CPCSEA), Ministry of Environment, Forests & Climate Change, Govt. of India. The experiments were performed in compliance with the relevant laws and guidelines of the CPCSEA.

Solid tumor production

The murine Sarcoma-180 cells used in this study were maintained *in vivo* by intraperitoneal passage of $2x10^6$ cells in male Swiss albino mice. Solid tumors were produced by subcutaneous inoculation of $1x10^6$ S-180 cells on the dorsal surface of right

RSC Advances Accepted Manuscript

hind leg of Swiss albino mice. Viability was assessed by the Trypan blue dye exclusion method.

Treatment

After seven days of tumor inoculation, anethole (10, 20 and 40 mg/kg body weight), dissolved in 50% ethanol, was administered orally by gavage every alternate day for 21 days after tumor inoculation.

Cyclophosphamide (100mg/kg b.w.) was administered intraperitoneally on alternate days from day 17 onwards.

Experimental groups

All the animals were randomly divided into five groups of 6 animals each: i) saline treated normal mice ii) Tumor bearing control mice (Sarcoma control) iii) Tumor bearing mice treated with 50% alcohol (alcohol control) iv) Tumor bearing animals treated with three doses of anethole (anethole 10, 20 and 40 mg/kg) iv) Tumor bearers treated with cyclo considered as the standard reference drug and v) Tumor bearers treated with a combination of cyclophosphamide and anethole (cyclo+anethole10/20/40mg/kg). Two additional experimental groups were also set up to prove the hepatoprotective effect of anethole, viz., vi) Mice treated with a standard hepatotoxic agent, CCl_4 vii) Mice pre-treated with anethole followed by CCl_4 administation. The weights of all the animals belonging to different groups were recorded weekly throughout the experimental period.

Sera Isolation

Mice were anesthetized with diethyl ether, and the blood was removed from the tail vein into tubes. Serum was separated from freshly collected blood by allowing it to clot at a slanting position for 45mins then centrifugation at 1,500 × *g* for 30 min at 4°C. Finally, serum samples were stored in aliquots at −20°C for later use. All serum samples were thawed once at the time of assay.

RSC Advances Accepted Manuscript

Measurement of Serum Biochemical Parameters

Alanine aminotransferase (ALT), aspartate aminotransferase (AST), alkaline phosphatase (AP), urea and creatinine levels were measured from collected sera using Autospan liver function test kit, Span Diagnostics Ltd., Surat, India.

Measurement of tumor volume and tumor weight

The antitumor activity was assessed by measuring tumor weight and the changes in tumor volume. Changes in tumor size over time after tumor transplantation was assessed in all the experimental groups. The length and width of the tumor were measured using calipers. Tumor volume was calculated by the following formula:

Tumor volume (mm^3): 0.5 x a x b^2 where a is the largest diameter and b its perpendicular.

Dissection and Tissue collection

All the mice were euthanized after the last dose of anethole treatment. Liver, kidneys, urinary bladders, femurs and tumor tissues of the animals from all the experimental groups were collected, washed in 0.9% saline, soaked in filter paper and processed for cellular, biochemical and histological studies.

Bone Marrow cell count

Femurs were aseptically removed from the treated and untreated tumor bearers. The bone marrow was then flushed with 26 gauge needles. Single cell suspensions were made with repeated aspirations. The cells were resuspended in RPMI-1640. The viable cell count was made in a hemocytometer by the Trypan Blue exclusion method.

Histopathological assessment

Tumor, liver, urinary bladder and kidney tissues were fixed overnight at 4°C in freshly prepared 4% paraformaldehyde and then dehydrated in graded alcohols and embedded in paraffin. Sections of 5 μm thickness were cut from representative paraffin blocks. Tumor tissues were cut right through the middle of the tissues to obtain the central core region. The sections were rehydrated and stained with hematoxylin and eosin. Stained

RSC Advances Accepted Manuscript

sections were observed under light microscope (Olympus CX41). The degree of liver damage on microscopic cross-sections was scored by a pathologist in a blinded fashion following a modified Brunt System[38]. Four histologic features: steatosis, hepatocyte ballooning, portal inflammation, and lobular inflammation were primarily taken into consideration to score the grade of liver damage. Sections of urinary bladder were evaluated to study the effect of anethole on urotoxicity induced by cyclo. Kidney sections were also scored by the pathologist based on presence or absence of tubular inflammation, glomerular changes and hyalinization.

Assay of Hepatic Lipid peroxidation (LPO)

The extent of LPO and liver homogenates was determined quantitatively by performing the method as described by Ohkawa et al., 1979[39]. The amount of malondialdehyde (MDA) was measured by reaction with thiobarbituric acid at 532 nm using spectrophotometer (Eppendorf BioSpectrometer Kinetic). MDA levels were calculated using the standard curve of MDA and its level expressed in nM/mg of protein.

Bone Marrow and Tumor Cell cycle distribution analysis

For the determination of cell cycle phase distribution of nuclear DNA, cells from bone marrow, spleen and tumor tissue ($1x10^6$cells) were harvested from tumor bearing untreated and treated mice. After making a single cell suspension, cells were fixed with 3% p-formaldehyde, permeabilized with 0.1% NP-40, and nuclear DNA was labeled with propidium iodide (PI, 125 μg/mL) after RNase treatment. Cell cycle phase distribution of nuclear DNA was determined on FACSVerse using FACSuite software (Becton-Dickinson). Histogram display of DNA content (x-axis, PI fluorescence) versus counts (y-axis) has been displayed. Cell Quest statistics was employed to quantitate the data at different phases of the cell cycle.

Detection of Mechanism of Cell Death

Annexin V Assay

RSC Advances Accepted Manuscript

Apoptosis assays were carried out based on the instruction from the Annexin V Apoptosis Kit. Briefly, PI and Annexin V were added directly to the single cell suspension of the tumor tissue. The mixture was incubated for 15 min at 37^{o}C. Cells were fixed and then analyzed on FACS Verse (Becton Dickinson). Electronic compensation of the instrument was done to exclude overlapping of the emission spectra. Total 10,000 events were acquired, the cells were properly gated and dual parameter dot plot of FL1-H (x-axis; Fluos-fluorescence) versus FL2-H (y-axis; PI-fluorescence) shown in logarithmic fluorescence intensity.

Single cell gel electrophoresis (SCGE, the Comet assay)

The alkaline version of the comet assay was performed in sarcoma, bone marrow and liver cells according to the method of Singh et al. 1988[40], with slight modifications. In brief, 25µL of the single suspension of the cells of interest are suspended in low melting agarose (LMA) 0.5%, in phosphate-buffered saline (PBS) and layered onto fully frosted microscope slides pre-coated with 480 µL of standard agarose 0.75% in PBS. A final layer of 100 µl of 0.5% LMA was added on top. Slides were immersed in a jar containing cold lysing solution (1% Triton X-100; 10% DMSO; 10mM Tris; 2.5M NaCl; 1mM Na_2EDTA with pH 10 at −4°C for 1h). Slides were pretreated for 20min in unwinding buffer (300mM NaOH; 1mM Na_2EDTA/pH 13. Electrophoresis was carried out using the same solution buffer for 20min/25V and 300 mA (0.8V/cm). Pre-incubation and electrophoresis were performed in an ice bath. Afterwards, the slides were washed three times in 0.4M Tris/pH 7.4, and DNA was stained by adding 20µL of ethidium bromide (10µg/mL). The slides were examined under a fluorescence microscope (Dewinter Victory Prime TR) at 400X magnification to count the number of comet cells per field in the samples of different experimental groups.

Western blot analysis

Cell lysates were obtained and equal amounts of protein from each sample were diluted with loading buffer, denatured, and separated by 10% sodium dodecyl sulfate-

RSC Advances Accepted Manuscript

polyacrylamide gel electrophoresis (SDS-PAGE) followed by protein transfer to polyvinylidene fluoride membranes (PVDF). The effect of treatment on the expression of certain proteins such as p53, p21, caspase-3, PARP-1, Bax, Bcl-2, caspase-8 and PCNA was determined. Proteins were detected by incubation with corresponding primary antibodies (anti p53, anti-p21, anti-capsase3, anti-PARP-1, anti-Bax, anti-Bcl-2, anti-caspase-8 and anti-PCNA) antibodies followed by blotting with HRP-conjugated secondary antibody. The blots were then detected by using a chemiluminescence kit (ImmunoCruz Western Blottimg Luminol reagent, sc-20489). This analysis was performed three times.

Statistical analysis

The experiments were repeated three times and the data were analyzed statistically. Values have been shown as standard error of mean, except where otherwise indicated. Data were analyzed and one-way ANOVA was used to evaluate the statistical differences. Tukey's multiple comparison test was then used to compare the difference between each pair of means. Statistical significance was considered when $p < 0.05$.

CONCLUSION

The results of this investigation indicate that anethole is a potent antitumor agent when administered singly or in combination with cyclo. The principal mechanism of cell death induced by cyclo was found to be necrosis while in case of anethole it is apoptosis. Interestingly, in the combination groups, the ratio of apoptosis to necrosis increased as compared to cyclo suggesting a change in the nature of cell death. Based on cell cycle, annexin V and protein expression studies, the cytotoxicity of the three treatment regime towards tumor cells was found to be in the following order: cyclo+anethole>cyclo>anethole. The results further prove that anethole is an effective protective agent against myelosuppression, liver damage and urinary bladder damage that resulted from the treatment with cyclo. The hepatoprotective activity of anethole was further proven by its ability to reduce CCl_4 induced liver necrosis in mice. Thus, anethole

RSC Advances Accepted Manuscript

pre-treatment ameliorated the side-effects of cyclo treatment without impairing its therapeutic activity in the S-180 transplantable tumor model.

ACKNOWLEDGMENT

This work has been funded by the Council for Scientific and Industrial Research (CSIR), Govt. of India (Scheme No. 37(1487)/11/EMR-II).

References:

1. A. Dolci, R. Dominici, D. Cardinale, M.T. Sandri and M. Panteghini, *Am J Clin Pathol*., 2008,**130**, 688-695.
2. J. Yu, *Transl Cancer Res.,* 2013, **2**, 384-396.
3. I.H, Plenderleith. *Can Fam Physician*., 1990, **36**,1827-1830.
4. J.P. Cosse and C. Michiels, *Anticancer Agents Med Chem.,* 2008, **8,** 790-797.
5. N.P. Gullett, A.R. Ruhul Amin, S. Bayraktar, J.M. Pezzuto, D.M. Shin, F.R. Khuri, B.B. Aggarwal, Y.J. Surh and O. Kucuk, *Semin Oncol.,* 2010, **37**, 258–281.
6. S.C. Gupta, J.H. Kim, S. Prasad and B.B. Aggarwal. *Cancer Metastasis Rev*., 2010, **29**, 405–434.
7. D.J. Newman, G.M. Cragg and K.M. Snader. *J Nat Prod*., 2003, **66**, 1022–1037.
8. M. D'Incalci, W.P. Steward and A.J. Gescher. *Lancet Oncol***.,** 2005, **6**, 899-904
9. S. Budavari, The Merck Index. An encyclopedia of chemicals, drugs, and biologicals. 11th ed. Rahway NJ: Merck & Co, Inc; 1996, pp. 108-9.
10. G.B. Chainy, S.K. Manna, M.M. Chaturvedi and B.B. Aggarwal, *Oncogene*.,2000, **9**, 2943-2950.
11. C.H. Chen and L.A. deGraffenried, *Phytomedicine.*, 2012, **19**, 763-767.
12. E.J. Choo, Y.H. Rhee, S.J. Jeong, H.J. Lee, H.S. Kim, H.S. Ko, J.H. Kim, T.R. Kwon, J.H. Jung, J.H. Kim, H.J. Lee, E.O. Lee, D.K. Kim, C.Y. Chen and S.H. Kim, *Biol Pharm Bull.,* 2011, **34**, 41-46.
13. Y.H. Rhee, P.S. Chung, S.H. Kim and J.C. Ahn, Biochem *Biophys Res Commun.,*2014, **447**,557-562.
14. B. Ha, H. Ko, B. Kim, E.J. Sohn, J.H. Jung, J.S. Kim, J.J. Yoon, G. Won, J.H. Kim, D.B. Jung, M. Yun, B. Shim and S.H. Kim, *J Nat Prod.,* 2014, **77**, 63-69.
15. M.M. al-Harbi, S. Qureshi, M. Raza, M.M. Ahmed, A.B. Giangreco and A.H. Shah, *Eur J Cancer Prev*., 1995, **4,** 307-318.
16. J.W. Ho and M.W. Cheung, *Recent Pat Anticancer Drug Discov*., 2014, **9**, 297-302.

RSC Advances Accepted Manuscript

17. N. Driessens, S. Versteyhe, C. Ghaddhab, A. Burniat, X. De Deken, J. Van Sande, J.E. Dumont, F. Miot, B. Corvilain, *Endocr Relat Cancer*., 2009, **16**, 845-856.

18. L. Shu, K.L. Cheung, T.O. Khor, C. Chen and A.N. Kong, *Cancer Metastasis Rev.,* 2010, **29**, 483-502.

19. H.A. Norman, R.R. Butrum, E. Feldman, D. Heber, D. Nixon, M.F. Picciano, R. Rivlin, A. Simopoulos, M.J. Wargovich and E.K. Weisburger, *J Nutr*., 2003, **133**, 3794S-3799S.

20. B. Sung, S. Prasad, V.R. Yadav, B.B. Aggarwal, *Nutr Cancer.,* 2012, **64**, 173-197.

21. M.U. Nessa, P. Beale, C. Chan, J.Q. Yu and F. Huq, *Anticancer Res.,* 2012, **32**, 4843-4850.

22. H.J. van der Woude, J.L. Bloem, P.C. Hogendoorn. Skeletal Radiol., 1998, 27, 57-71.

23. W.L. Monsky, B. Jin, C. Molloy, R.J. Canter, C.S. Li, T.C. Lin, D. Borys, W. Mack, I. Kim, M.H. Buonocore, A.J. Chaudhari. Anticancer Res., 2012, 32, 4951-4961.

24. A. M. Kaiser, A. K. Saluja, A. Sengupta, M. Saluja, M. L. Steer, *Am J Physiol*., 1995, **269,** C1295-C1304.

25. D. W. Lamson and M. S. Brignall, *Alternative Medicine Review.,* 1999, **4**, 304–329.

26. S. Golbidi, A. Botta, S. Gottfred, A. Nusrat, I. Laher, S. Ghosh, *Br J Pharmacol*., 2014, **171**, 5345-5360.

27. D.R. McIlwain, T. Berger and T.W. Mak, *Cold Spring Harb Perspect Biol*., 2013, **5**, a008656.

28. M.A. O'Donnell, E. Perez-Jimenez, A. Oberst, A. Ng, R. Massoumi, R. Xavier, D.R. Green, A.T. Ting. *Nat Cell Biol.,* 2011, **13**, 1437-1442.

29. A. Oberst, C.P. Dillon, R. Weinlich, L.L. McCormick, P. Fitzgerald, C. Pop, R. Hakem, G.S. Salvesen, D.R. Green. *Nature.,* 2011, **471**, 363-367.

30. C.M. Galmarini, N. Voorzanger, N. Falette, L. Jordheim, E. Cros, A. Puisieux and C. Dumontet, *Biochem Pharmacol*., 2003, **65**, 121-129.

31. C.L. Edelstein, Y. Shi and R.W. Schrier, *J Am Soc Nephrol,* 1999, **10**, 1940-1949.

32. S. Gobeil, C.C. Boucher, D. Nadeau and G.G. Poirier, *Cell Death Differ*., 2001, **8** 588-594.

33. N. Kaplowitz, *Clin Infect Dis.,* 2004, **38**, Suppl 2:S44-8.

34. D.T. Vincent, Y.F. Ibrahim, M.G. Espey and Y.J. Suzuki, *Cancer Chemother Pharmacol.,* 2013, **72,** 1157-1168.

35. P. Pratheesh Kumar and G. Kuttan, *Inflammopharmacology.,* 2010,**18**, 197-207

RSC Advances Accepted Manuscript

36. F. Senatore, F. Oliviero, E. Scandolera, O. Taglialatela-Scafati, G. Roscigno, M. Zaccardelli and E. De Falco, *Fitoterapia*., 2013, **90**, 214-219.

37. R.S. Freire, S.M. Morais, F.E. Catunda-Junior and D.C. Pinheiro, *Bioorg Med Chem*., 2005, **13**, 4353-4358.

38. S. Merat, F. Khadem-Sameni, M. Nouraie, M.H. Derakhshan, S.M. Tavangar, S. Mossaffa, R. Malekzadeh and M. Sotoudeh, *Arch Iran Med*., 2010, **13**, 38 – 44.

39. H. Ohkawa, N. Oshisi and K. Yagi, *Anal Biochem*., 1979, **95**, 351–358.

40. N. P. Singh, M. T. McCoy, R.R. Tice and E.L. Schneider, *Exp Cell Res*., 1988, **175,** 184–191.

Figure Legends

Fig 1. Antitumor potential of various doses of Anethole A) Change in tumor weight. Data represented in bar diagrams of mean $\pm$ SD of three independent experiments. Significant difference ($p<0.05$) is indicated with the following symbols "*"when compared with Sarcoma control; "Φ" when compared between Anethole 10 and 20; "Δ"when compared between Anethole 20 and 40. B) Micrograph of representative H-E stained sections tumor tissue showing diffused necrotic zone in the treated groups (indicated by arrows).

Fig 2. Induction of Apoptosis by Anethole in S-180 cells A) Annexin V/PI Assay in S-180 cells. In a double label system, unfixed S-180 cells from tumor-bearing treated and untreated mice were labeled with PI and Annexin V and then fixed and analyzed on a Flowcytometer. B) Graphical representation of percentage necrotic (white area) and apoptotic cells (gray area) by indicated doses of anethole. C) Representative photo micrographs of comet cells. Alkaline single cell gel electrophoresis was performed and the number of 'comet' cells per field was counted under a fluorescent microscope. D) Graphical representation of percentage comet formation in the indicated experimental groups. The data represented as mean+ S.D. for the three different experiments performed in triplicate. Significant difference ($p<0.05$) is indicated with the following

RSC Advances Accepted Manuscript

symbols "*"when compared with Sarcoma control; "Φ" when compared between Anethole 10 and 20; "Δ"when compared between Anethole 20 and 40..

Fig 3. Effect of anethole on other organs. A) Micrograph of representative H-E stained sections of liver B) Graphical representation of liver histology scoring which was done based on the extent of steatosis, hepatocyte ballooning, portal and lobular inflammation. C) The levels of LPO in the tumor tissue homogenates as determined quantitatively by reaction with thiobarbituric acid at 532 nm using spectrophotometer and expressed as nM MDA/mg protein. D) Micrograph of representative H-E stained sections of kidney E) Tabular representation of kidney histology scoring based on inflammatory infiltration, hyalinization, glomerular changes and tubular swelling. NA signifies mentioned features not observed and YES signifies presence of such features F) Graphical representation of bone marrow cell count of different groups. Cells were flushed from 1cm femur with 26 gauge needles. The viable cell count was made in a hemocytometer by the Trypan Blue exclusion method. The data represented as mean±S.D. for the three different experiments performed in triplicate. Significant difference ($p<0.05$) is indicated with the following symbols "†"when compared with Normal; "*"when compared with Sarcoma control; "Φ" when compared between Anethole 10 and 20; "Δ"when compared between Anethole 20 and 40 and "*" indicates $p<0.05$ when compared with Sarcoma control.

Fig 4. Antitumor activity of cyclo and combination groups. A) Change in tumor weight B) Change in Tumor volume. C) Micrograph of representative H-E stained sections tumor tissue showing necrotic zones in the treated groups (indicated by arrows). The data represented as mean+S.D. for the three different experiments performed in triplicate. Significant difference ($p<0.05$) is indicated with the following symbols"*"when compared with Sarcoma control; "‡" when compared with Cyclo; "ψ"

RSC Advances Accepted Manuscript

when compared between Cyclo + Anethole 10 and Cyclo + Anethole 20 and "∓" when compared between Cyclo + Anethole 20 and Cyclo + Anethole 40.

Fig 5. Differential nature of cell death induced by cyclo and anethole: A) S-180 tumor cell cycle phase distribution detected in a flowcytometer. Histogram display of DNA content (*x*-axis, PI-fluorescence) vs. counts (*y*-axis) has been shown. B) Bar diagram representation of cell cycle phase distribution of S-180 from different experimental groups. C) Annexin V/PI Assay of tumor cells. Dual parameter dot plot of FITC-fluorescence (*x*-axis) vs. PI-fluorescence (*y*-axis) has been shown in logarithmic fluorescence intensity. In a double label system, unfixed S-180 cells from tumor-bearing treated and untreated mice were labeled with PI and Annexin V and analyzed on a Flowcytometer. D) Bar diagram representation of percent Annexin V positive, PI positive and dual positive S-180 cells from different experimental groups. E) Graphical representation of percentage necrotic (white area) and apoptotic cells (black area) induced by the indicated treatment regimes. Data represented in bar diagrams of mean ± SD of 3 independent experiments. Significant difference ($p<0.05$) is indicated with the following symbols"*"when compared with Sarcoma control; "‡" when compared with Cyclo; "ψ" when compared between Cyclo + Anethole 10 and Cyclo + Anethole 20 and "∓" when compared between Cyclo + Anethole 20 and Cyclo + Anethole 40.

Fig. 6. Effect of all the treatment regimes on tumor tissue protein expressions by Western Blot analysis. Representative blots of A) p53 B) p21 C) PARP-1 D) Bax E) Bcl-2 F) Bax/Bcl-2 ratio G) caspase-3 H) caspase-8 I) PCNA. Equal loading of protein in the lanes was confirmed by GAPDH (J). Densitometric analysis of the blots are represented in bar diagrams of mean ± SD of three independent experiments; Significant difference ($p<0.05$) is indicated with the following symbols"*"when compared with Sarcoma control; "‡" when compared with Cyclo; "Φ" when compared between Anethole 10 and 20; "Δ"when compared between Anethole 20 and 40, "ψ" when

RSC Advances Accepted Manuscript

compared between Cyclo + Anethole 10 and Cyclo + Anethole 20 and "╤" when compared between Cyclo + Anethole 20 and Cyclo + Anethole 40.

Fig.7. Toxicities of various treatment modalities. A) Bone marrow cell count. B) Graphical representation of flowcytometric cell cycle phase distribution of bone marrow cells from different experimental groups C) Representative photo micrographs of comet cells in bone marrow. D) Graphical representation of percentage comet formation in the bone marrow of indicated experimental groups. E) Micrograph of representative H-E stained sections of liver from cyclo and combination of cyclo+anethole F) Graphical representation of liver histology scoring which was done based on the extent of steatosis, hepatocyte ballooning, portal and lobular inflammation. G) Representative liver sections from mice treated with CCl_4 or carbon tetrachloride plus Anethole 20. H) Necrotic zones were quantified by counting unit areas. A field was divided equally into 165 square units. Necrosis or Viable zones were counted and represented as percentage. Mean ± SD were calculated from a survey of 20 fields from each slide and represented as histogram bars. I) Representative photo micrographs of comet cells in liver. J) Graphical representation of percentage comet formation in liver of indicated experimental groups. K) Micrograph of representative H-E stained sections of urinary bladder L) Tabular representation of urinary bladder histology scoring based on degenerative transitional epithelium and inflammation. The data represented as mean ± S.D. for the three different experiments performed in triplicate. Significant difference ($p<0.05$) is indicated with the following symbols "†"when compared with Normal, "*"when compared with Sarcoma control; "‡" when compared with Cyclo; "ψ" when compared between Cyclo + Anethole 10 and Cyclo + Anethole 20 and "╤" when compared between Cyclo + Anethole 20 and Cyclo + Anethole 40.

RSC Advances Accepted Manuscript

Table1: Serum biochemical parameters of hepatotoxicity in different experimental groups

	Parameters	Normal	Sarcoma Control	Alcohol Control	Cyclo	Cyclo+A10	Cyclo+A20	Cyclo+A40	CCl_4	CCl_4+A20
Liver Function Test (U/mL)	ALT	18.05±0.83	34.11±2.45	36.35±1.88	44.26±1.69	33.615±3.07	23.027±0.76	84.65±1.74	105 ± 3.22	91.8 ± 1.66
	AST	21.033±0.78	79.74±4.12	81±3.22	85.93±1.44	74.32±2.44	76.06±1.87	79.6±3.89	120 ± 2.11	95 ± 1.88
	AP	31.23±2.08	45.11±1.89	47±2.22	69.03±2.05	59.96±1.23	54.79±0.77	50.65±2.43	93 ± 3.22	51 ± 3.04

Data are given as means ± SD.

RSC Advances Accepted Manuscript

Table 2: Serum biochemical parameters of renal toxicity in different experimental groups

	Parameters	Normal	Sarcoma Control	Alcohol Control	Cyclo	Cyclo+A10	Cyclo+A20	Cyclo+A40
Renal Function Test (mg/dL)	Urea	29.25±0.95	32.75±1.71	34 ± 1.5	48.25±2.50	33.75±1.29	37.50±1.29	41.25±0.96
	Creatinine	0.98±0.03	1.14±0.06	1.16 ± 0.04	1.60±0.105	1.15±0.04	1.18±0.08	1.19±0.032

Data are given as means ± SD.

RSC Advances Accepted Manuscript

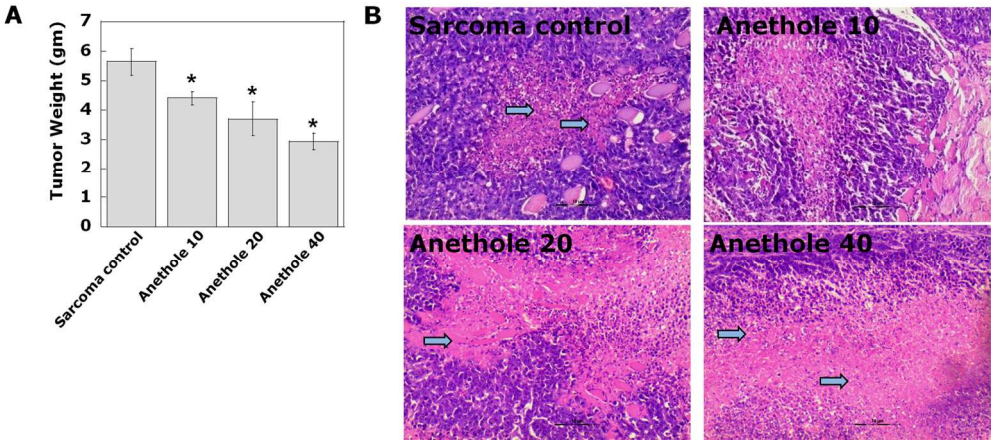

Antitumor potential of various doses of Anethole A) Change in tumor weight. Data represented in bar diagrams of mean + SD of three independent experiments. Significant difference ($p<0.05$) is indicated with the following symbols "*"when compared with Sarcoma control; "Φ" when compared between Anethole 10 and 20; "Δ"when compared between Anethole 20 and 40. B) Micrograph of representative H-E stained sections tumor tissue showing diffused necrotic zone in the treated groups (indicated by arrows).

RSC Advances Accepted Manuscript

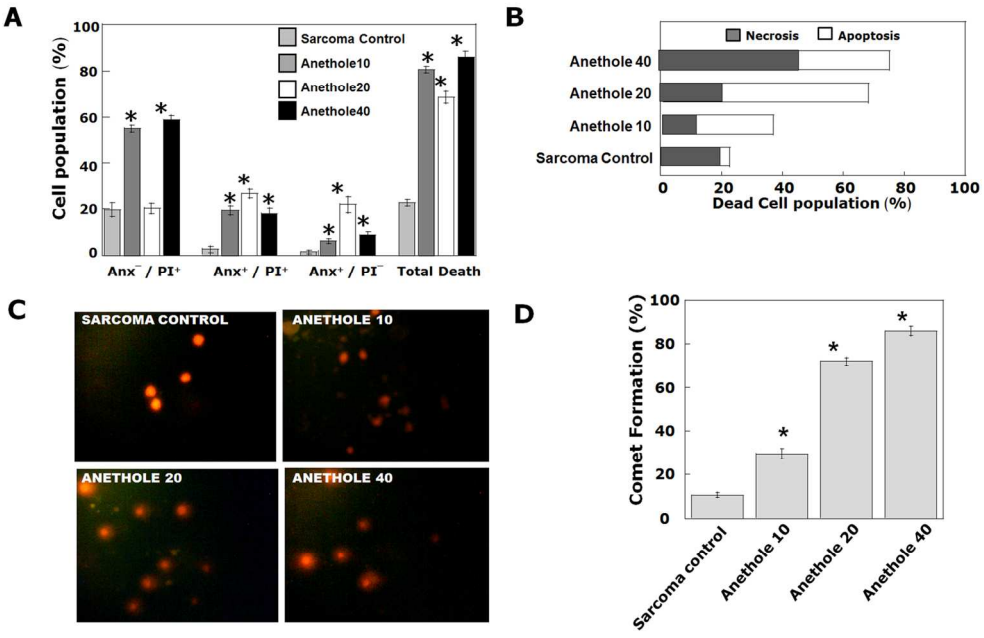

Induction of Apoptosis by Anethole in S-180 cells A) Annexin V/PI Assay in S-180 cells. In a double label system, unfixed S-180 cells from tumor-bearing treated and untreated mice were labeled with PI and Annexin V and then fixed and analyzed on a Flowcytometer. B) Graphical representation of percentage necrotic (white area) and apoptotic cells (gray area) by indicated doses of anethole. C) Representative photo micrographs of comet cells. Alkaline single cell gel electrophoresis was performed and the number of 'comet' cells per field was counted under a fluorescent microscope. D) Graphical representation of percentage comet formation in the indicated experimental groups. The data represented as mean+ S.D. for the three different experiments performed in triplicate. Significant difference ($p<0.05$) is indicated with the following symbols "*"when compared with Sarcoma control; "Φ" when compared between Anethole 10 and 20; "Δ"when compared between Anethole 20 and 40.

RSC Advances Accepted Manuscript

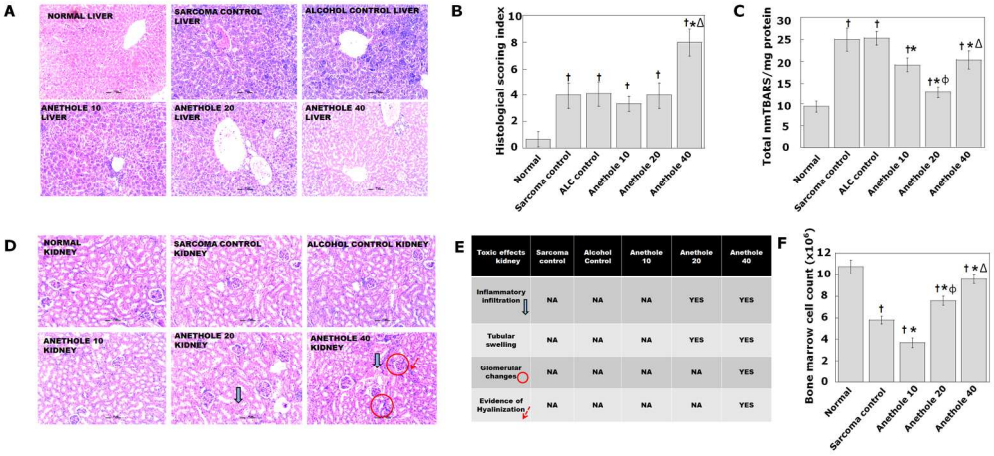

Toxic effects kidney	Sarcoma control	Alcohol Control	Anethole 10	Anethole 20	Anethole 40
Inflammatory infiltration	NA	NA	NA	YES	YES
Tubular swelling	NA	NA	NA	YES	YES
Glomerular changes	NA	NA	NA	NA	YES
Evidence of Hyalinization	NA	NA	NA	NA	YES

Effect of anethole on other organs. A) Micrograph of representative H-E stained sections of liver B) Graphical representation of liver histology scoring which was done based on the extent of steatosis, hepatocyte ballooning, portal and lobular inflammation. C) The levels of LPO in the tumor tissue homogenates as determined quantitatively by reaction with thiobarbituric acid at 532 nm using spectrophotometer and expressed as nM MDA/mg protein. D) Micrograph of representative H-E stained sections of kidney E) Tabular representation of kidney histology scoring based on inflammatory infiltration, hyalinization, glomerular changes and tubular swelling. NA signifies mentioned features not observed and YES signifies presence of such features F) Graphical representation of bone marrow cell count of different groups. Cells were flushed from 1cm femur with 26 gauge needles. The viable cell count was made in a hemocytometer by the Trypan Blue exclusion method. The data represented as mean+S.D for the three different experiments performed in triplicate. Significant difference ($p<0.05$) is indicated with the following symbols "†"when compared with Normal; "*"when compared with Sarcoma control; "Φ" when compared between Anethole 10 and 20; "Δ"when compared between Anethole 20 and 40 and "*" indicates $p<0.05$ when compared with Sarcoma control.

RSC Advances Accepted Manuscript

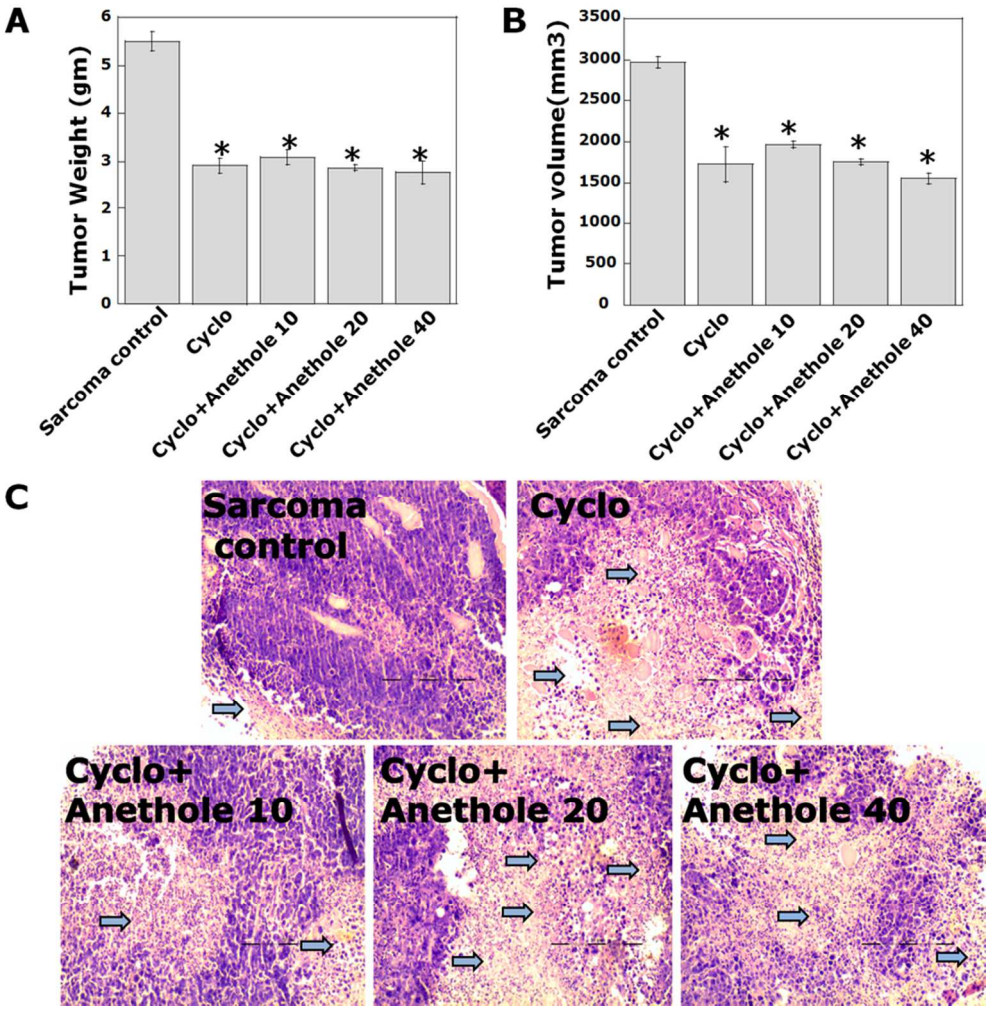

Antitumor activity of cyclo and combination groups. A) Change in tumor weight B) Change in Tumor volume. C) Micrograph of representative H-E stained sections tumor tissue showing necrotic zones in the treated groups (indicated by arrows). The data represented as mean+S.D. for the three different experiments performed in triplicate. Significant difference ($p<0.05$) is indicated with the following symbols"*"when compared with Sarcoma control; "‡" when compared with Cyclo; "ψ" when compared between Cyclo + Anethole 10 and Cyclo + Anethole 20 and "∓" when compared between Cyclo + Anethole 20 and Cyclo + Anethole 40.

RSC Advances Accepted Manuscript

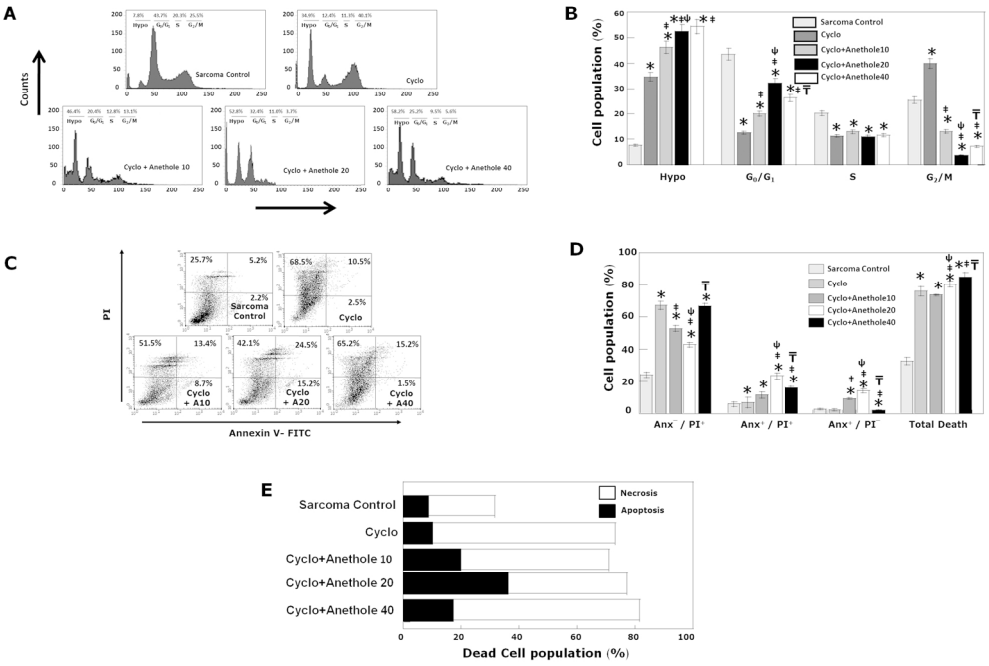

Differential nature of cell death induced by cyclo and anethole: A) S-180 tumor cell cycle phase distribution detected in a flowcytometer. Histogram display of DNA content (x-axis, PI-fluorescence) vs. counts (y-axis) has been shown. B) Bar diagram representation of cell cycle phase distribution of S-180 from different experimental groups. C) Annexin V/PI Assay of tumor cells. Dual parameter dot plot of FITC-fluorescence (x-axis) vs. PI-fluorescence (y-axis) has been shown in logarithmic fluorescence intensity. In a double label system, unfixed S-180 cells from tumor-bearing treated and untreated mice were labeled with PI and Annexin V and analyzed on a Flowcytometer. D) Bar diagram representation of percent Annexin V positive, PI positive and dual positive S-180 cells from different experimental groups. E) Graphical representation of percentage necrotic (white area) and apoptotic cells (black area) induced by the indicated treatment regimes. Data represented in bar diagrams of mean ± SD of 3 independent experiments. Significant difference ($p<0.05$) is indicated with the following symbols"*"when compared with Sarcoma control; "‡" when compared with Cyclo; "ψ" when compared between Cyclo + Anethole 10 and Cyclo + Anethole 20 and "╤" when compared between Cyclo + Anethole 20 and Cyclo + Anethole 40.

RSC Advances Accepted Manuscript

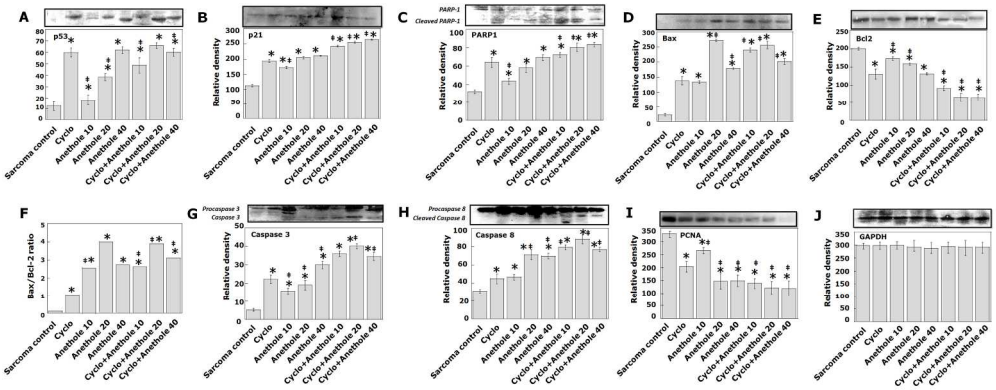

Effect of all the treatment regimes on tumor tissue protein expressions by Western Blot analysis. Representative blots of A) p53 B) p21 C) PARP-1 D) Bax E) Bcl-2 F) Bax/Bcl-2 ratio G) caspase-3 H) caspase-8 I) PCNA. Equal loading of protein in the lanes was confirmed by GAPDH (J). Densitometric analysis of the blots are represented in bar diagrams of mean + SD of three independent experiments; Significant difference ($p<0.05$) is indicated with the following symbols"*"when compared with Sarcoma control; "‡" when compared with Cyclo; "Φ" when compared between Anethole 10 and 20; "Δ"when compared between Anethole 20 and 40, "ψ" when compared between Cyclo + Anethole 10 and Cyclo + Anethole 20 and "╤" when compared between Cyclo + Anethole 20 and Cyclo + Anethole 40.

RSC Advances Accepted Manuscript

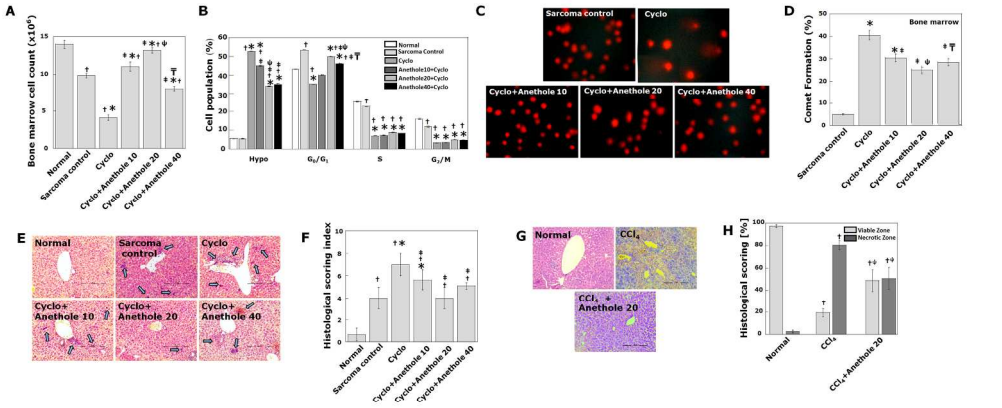

L

	Transition epithelial layer	Smooth muscle	Immuno cells infiltration
Normal	Normal	Normal	Nil
Sarcoma control	Normal	Normal	Nil
Cyclo	Degenerative	Degenerative	Present
A10 + Cyclo	Degenerative	Normal	Nil
A20+ Cyclo	Less Degenerative	Normal	Nil
A40+ Cyclo	Less Degenerative	Normal	Nil

Toxicities of various treatment modalities. A) Bone marrow cell count. B) Graphical representation of flowcytometric cell cycle phase distribution of bone marrow cells from different experimental groups C) Representative photo micrographs of comet cells in bone marrow. D) Graphical representation of percentage comet formation in the bone marrow of indicated experimental groups. E) Micrograph of representative H-E stained sections of liver from cyclo and combination of cyclo+anethole F) Graphical representation of liver histology scoring which was done based on the extent of steatosis, hepatocyte ballooning, portal and lobular inflammation. G) Representative liver sections from mice treated with CCl4 or carbon tetrachloride plus Anethole 20. H) Necrotic zones were quantified by counting unit areas. A field was divided equally into 165 square units. Necrosis or Viable zones were counted and represented as percentage. Mean ± SD were calculated from a survey of 20 fields from each slide and represented as histogram bars. I) Representative photo micrographs of comet cells in liver. J) Graphical representation of percentage comet formation in liver of indicated experimental groups. K) Micrograph of representative H-E stained sections of urinary bladder L) Tabular representation of urinary bladder histology scoring based on degenerative transitional epithelium and inflammation. The data represented as mean ± S.D. for the three different experiments performed in triplicate. Significant difference ($p<0.05$) is indicated with the following symbols "+"when compared with Normal, "*"when compared with Sarcoma control; "ǂ" when compared with Cyclo; "ψ" when compared between Cyclo + Anethole 10 and Cyclo + Anethole 20 and "∓" when compared between Cyclo + Anethole 20 and Cyclo + Anethole 40.

RSC Advances Accepted Manuscript